CHAPTER IV
RESULTS AND DISCUSSION

4.1 Nanocasting Process

4.1.1 Effect of Cerium Oxide Percentage by Weight

The effect of cerium oxide percentage by weight was studied by varying the % weight at 50, 60, 70, and 80%. Figure 4.1 shows the low angle XRD patterns of ordered mesoporous ceria and MCM-48, inset. The XRD pattern of MCM-48 shows reflection peaks at {211}, {220}, {420}, and {332}, consistent to our previous work (Longloilert *et al.*, 2011), corresponding to the Ia3d cubic structure. The ordered mesoporous (MSP) ceria (Fig. 4.1 a, b, c), the negative replica of the MCM-48 template, show the same characteristic diffraction peaks at {211} and {220} as the silica template whereas Fig. 4.1 d shows only one peak at {211}. These results suggest that the ceria replicas still retain some order from their template. The XRD pattern of the 50% weight of ceria shows higher intensity and sharper peak than those of 60, 70, and 80% weight of ceria, respectively, due to agglomeration of ceria in the pore channel of MCM-48 from the higher ceria loading during casting process. Moreover, the intensity of the ordered mesoporous ceria shows lower intensity than the MCM-48, indicating less order of the replica than the template.

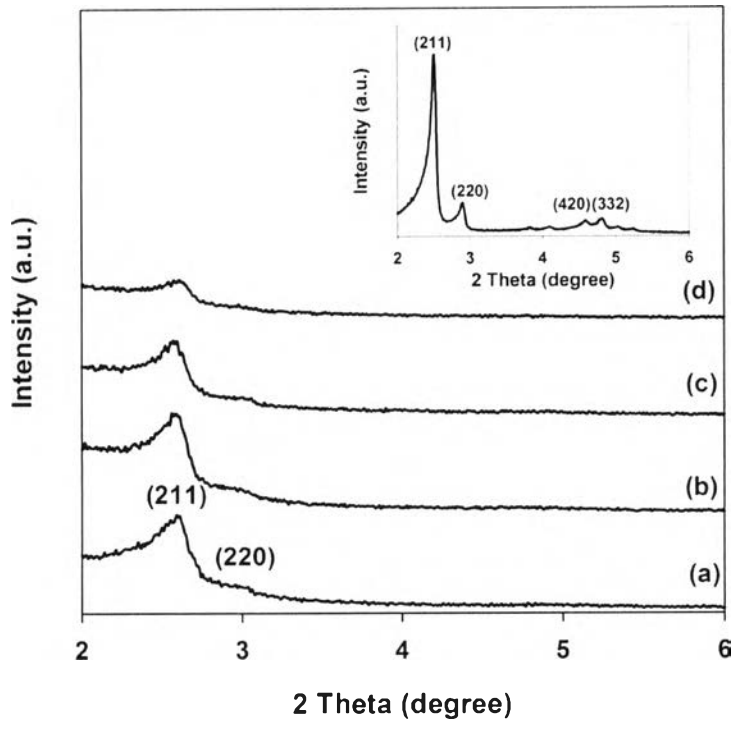

Figure 4.1 XRD patterns of MCM-48 (inset) and the ordered mesoporous ceria at a) 50; b) 60; c) 70; and d) 80% weight of ceria.

Surface area of the ordered mesoporous ceria was analyzed using nitrogen adsorption desorption isotherm and is listed in Table 4.1. As seen from the table, specific surface area decreased with increasing the % weight of ceria. Among them, the 50% weight shows the highest surface area. These results could be confirmed by the XRD results (Fig. 4.1), indicating the obstruction of ceria inside the pores (Liotta *et al.*, 2010), causing the ordered structure to be destroyed. The XRD pattern of 50% weight shows the sharpest diffraction peak and highest intensity, meaning that its replica was more crystalline and more ordered than the remains, thus providing high surface area (234.3 m^2 /g) whereas the XRD pattern of 80% weight showed a broad peak, indicating amorphous and exhibiting that the replica could not maintain the structure of MCM-48. Thus, the best ceria percentage to obtain a high surface area with maintaining MCM-48 structure is 50% and used for further study.

Table 4.1 Specific surface area of the ordered mesoporous ceria at different weight percentages

Ordered mesoporous ceria (% weight of ceria)	**Surface area (m^2/g)**
50	234.3
60	192.6
70	166.5
80	128.6

4.1.2 Effect of Stirring Time of Mixture

The effect of stirring time (30 min, 1, 2, and 4 h) of the precursor and the template in solvent was studied using 50% weight of ceria. The obtained XRD patterns of all ordered mesoporous ceria are shown in Fig. 4.2, exhibiting diffraction peaks at {211} and {220}, as shown for MCM-48. The intensity of the peak at {211} decreased with increasing the stirring time due to more amounts of the precursors went inside the pore and agglomerated, resulting in the less ordered structure at 4 h stirring time (Liotta *et al.*, 2010). These results indicate that the ordered mesoporous ceria at 30 min stirring time had the most ordered structure.

A decrease of specific surface area with increasing the stirring time is listed in Table 4.2. High surface area was obtained at 30 min stirring time, consistent with the XRD results. The longer period of stirring time allowed more precursors to infiltrate and block or agglomerate inside the pore of MCM-48 (Liotta *et al.*, 2010). Thus, the obtained ceria at the longer time of stirring became less ordered, resulting in a lower surface area. To this point, the appropriate condition of stirring time is at 30 min.

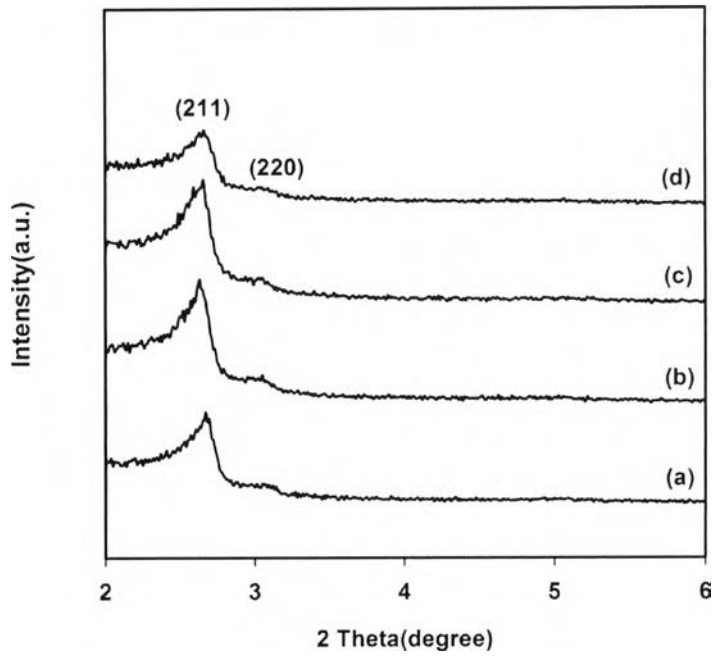

Figure 4.2 XRD patterns of the ordered mesoporous ceria at a) 30 min; b) 1; c) 2; and d) 4 h stirring time.

Table 4.2 Specific surface area of the ordered mesoporous ceria at different stirring times in the nanocasting process

Ordered MSP CeO_2 (stirring time)	**Surface area (m^2/g)**
30 min	246.6
1 h	241.4
2 h	213.9
4 h	214.0

4.1.3 Effect of Evaporated Temperature of Solvent

The effect of the evaporated temperature of solvent was studied because the precursor inside the pore void was expected to migrate and impregnate inside the pore during the evaporation of solvent (Yue *et al.*, 2008). Thus, how fast the precursor moved or penetrated depended on the evaporated temperature. The solvent in this process was ethanol, having boiling point around 78 °C, then the

temperatures studied were at ambient temperature, 50°, and 100 °C. The XRD patterns of the ordered mesoporous ceria are shown in Fig. 4.3, also giving the diffraction peaks at {211} and {220} although the ambient temperature showed less ordered than the others having with nearly the same intensity. It can be concluded that all the structure of the MCM-48 still retained and the studied range of the temperature had no influence on the migration of the precursor inside the pore.

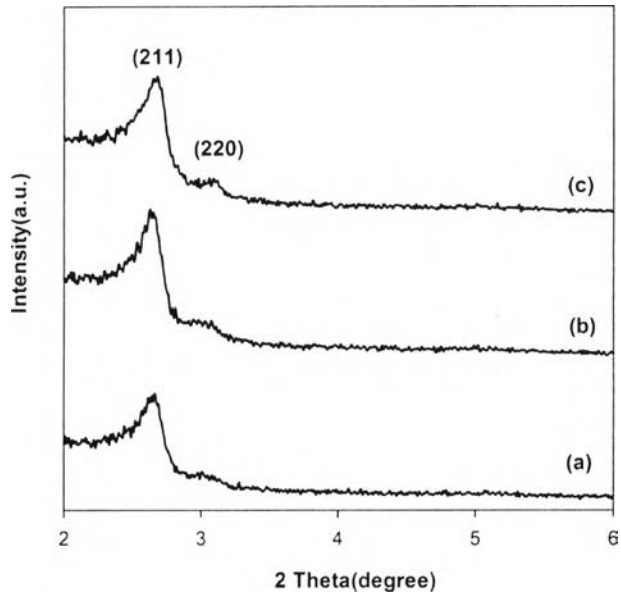

Figure 4.3 XRD patterns of the ordered mesoporous ceria at a) ambient; b) 50°; and c) 100 °C evaporated temperature in the nanocasting process.

Surface area results of those three evaporated samples at different temperature are in agreement with the XRD results such that the sample evaporated at ambient temperature provided the least surface area (211.8m^2/g), as can be seen in Table 4.3. The highest surface area (254m^2/g) was obtained from the sample evaporated at 100 °C. The reason probably comes from the fact that at 100 °C the evaporation time taken was the shortest around 1 hour while the evaporation time at ambient was the longest (2 days), meaning that the precursor had the longest time to migrate into inside the pore at the ambient temperature, causing the pore blocking

and the mesoporous structure to distort, as indicated less ordered in the XRD pattern (Horikawa *et al.*, 2011). Then the suitable evaporated temperature in this study was at 100 °C since it took the shortest time to evaporate the solvent out from the template while retaining the structure of the template and showing the highest surface area.

Table 4.3 Specific surface area of the ordered mesoporous ceria at different evaporated temperatures

Ordered mesoporous ceria (evaporated temperature)	**Surface area (m^2/g)**
RT.	211.8
50 °C	238.4
100 °C	254.0

4.1.4 Effect of Filling Cycle

In nanocasting process, the precursor cannot completely fill vacancies of the template at the first filling cycle due to the volume contraction rate (Hui *et al.*, 2010). The volume contraction occurs when the density of the final products is not close to the precursor. Thus, the effect of the filling cycle was studied by using 50% weight of cerium precursor, 30 min stirring time, and 100 °C evaporated temperature to remove the solvent during the nanocasting process.

The XRD results (Fig. 4.4) also show the diffraction peaks at {211} and {220}, referring to the MCM-48 structure, meaning that the structure of the template still retained although the filling cycle was increased. The XRD peaks obtained from 3 filling cycles (Fig. 4.4c) exhibit the sharpest diffraction peaks at {211} and {220} when comparing to the others. At the first filling cycle, the pore voids of the template were partly filled by the precursor, leaving some vacancies the template. The remaining vacancies were fulfilled further by the second and the third filling cycles. The sharpest peak was achieved at the 3 time filling cycles, suggesting that it duplicated better structure of the template than the others. Another word, it has

more ordered structure. This result confirms that a repeated filling cycle can effectively increase the filling degree, as described by Qian *et al.* in 2007.

To confirm the crystalline of the ceria, wide-angle of XRD was investigated. The XRD patterns (Fig. 4.5) show peaks at 2θ = 29°, 33.2°, 47.2°, 56.3°, 59.1°, 69.3°, 76.8°, and 78.9°, belonging to the peaks of the cubic fluorite structured ceria (Aranda *et al.*, 2009). Moreover, the XRD peak at 2θ = 22°, attributed to amorphous silica, was not detected in the ordered mesoporous cerium oxide (final product), indicating that the silica template, might be removed from the final product (Roggenbuck *et al.*, 2007).

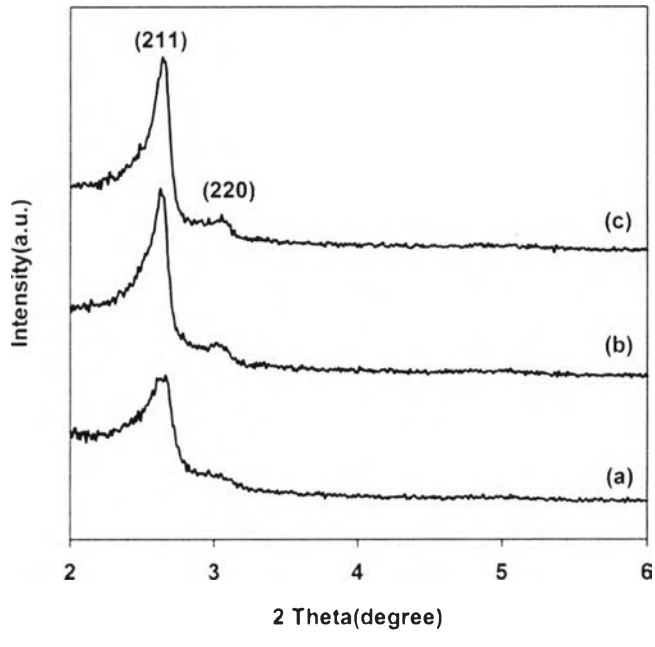

Figure 4.4 XRD patterns of the ordered mesoporous ceria at a) 1; b) 2, and c) 3 filling cycles.

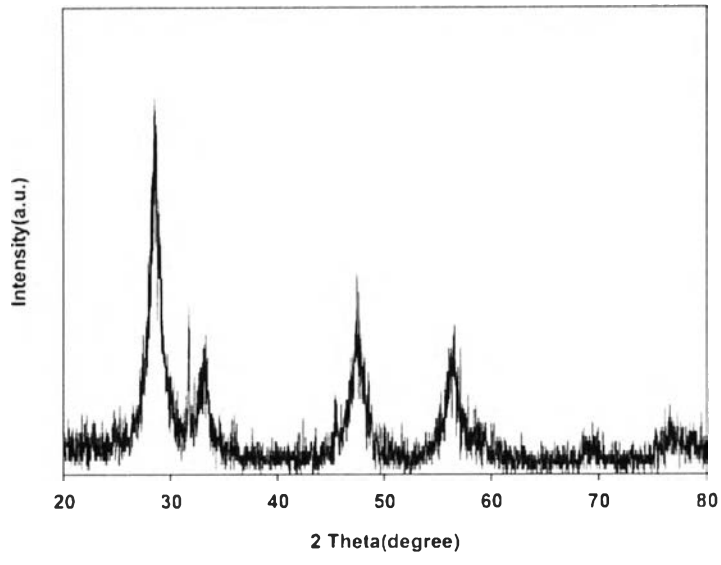

Figure 4.5 Wide-angle XRD of the ordered mesoporous ceria.

The presence of the silica template was confirmed further using XRF technique, and the results summarized in Table 4.4 indicate that small amount of Si still remained in the ordered mesoporous ceria after removal of the template.

Table 4.4 XRF analysis of ordered mesoporous ceria

Ordered mesoporous ceria (Filling cycles)	Ce (%)	O (%)	Si (%)
1	54.526	43.541	1.933
2	58.791	38.764	2.445
3	53.415	44.395	2.190

N_2 adsorption-desorption isotherms of the ordered mesoporous ceria (Fig. 4.6) were analyzed and found that the claasification of the synthesized ceria was a type IV isotherm with H3 hysteresis loop, IUPAC classification, corresponding to mesoporous materials with slit-like pores. The isotherms show the first step up at P/Po = 0.5-0.7 corresponding to the capillary condensation and the other step at P/Po = 0.9-1.0 reflecting the interparticle porosity (Shen, *et al*, 2005). The pore size

distribution curve (Fig. 4.6, inset) shows the sharp peak with the pore diameter around 5 nm which confirms the ordered mesoporous ceria contains uniform pores.

Table 4.5 is a list of BET surface area, pore volume, and pore size which were analyzed using nitrogen adsorption desorption isotherm. With the increasing filling cycle, the BET specific surface area and the pore volume were all decreased, meaning that ceria has infiltration into the template pore (Shen, *et al.* 2005). The pore size of the ordered mesoporous ceria, calculated from the desorption branch of the isotherm using the BJH method, is in a range of 4.5–4.8 nm which is larger than the wall thickness of MCM-48 (1.53 nm). This could indicate that the fillings of the pores probably overlapped in some region of the template (Ying, *et al*, 2011). As can be seen from Table 4.5, the highest surface area of the ordered mesoporous ceria obtained was 224.7m^2/g at 1 filling cycle. The other ceria products were still larger than the calcined ceria directly from the precursor at 823 K for 6 h.

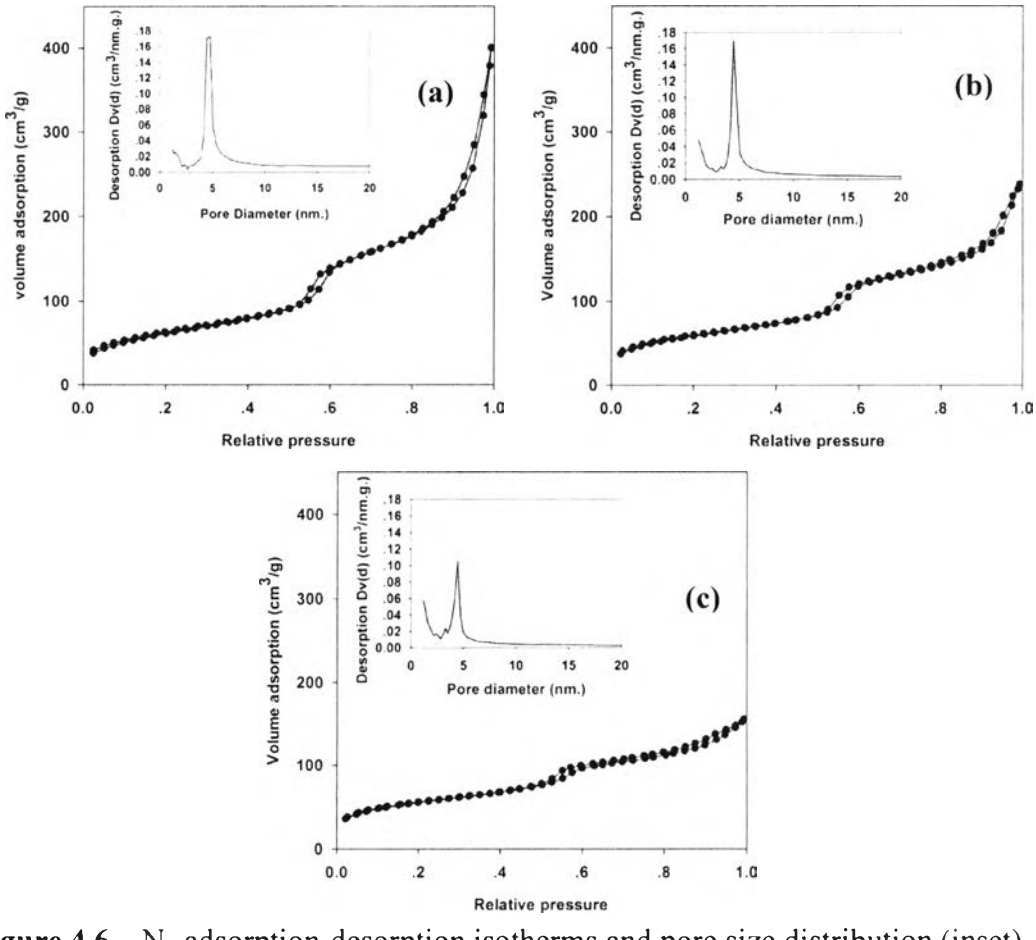

Figure 4.6 N_2 adsorption-desorption isotherms and pore size distribution (inset) of the ordered mesoporous ceria at a) 1; b) 2; and c) 3 filling cycles.

Table 4.5 Specific surface area, pore volume and pore size of MCM-48, CeO_2 and ordered mesoporous ceria at different filling cycles

Sample	Surface area (m^2/g)	Pore volume (cm^3/g)	Pore size (nm)
MCM-48	1614	1.1	2.5
Ceria powder	77.1	-	-
Ordered MSP Ceria (1 filling cycle)	224.7	0.6	4.8
Ordered MSP Ceria (2 filling cycles)	207.9	0.4	4.5
Ordered MSP Ceria (3 filling cycles)	192.0	0.2	4.5

SEM images of ceria and ordered mesoporous ceria are shown in Fig. 4.7. The ordered mesoporous ceria, Fig. 4.7 b, has spherical morphology which comprises of small round crystalline of ceria. Interestingly, the more filling cycles resulted in the denser spherical morphology of the ordered mesoporous ceria (Fig. 4.7 c, d). The SEM results can be well related to the surface area results that the denser spherical morphology gave the lower surface area.

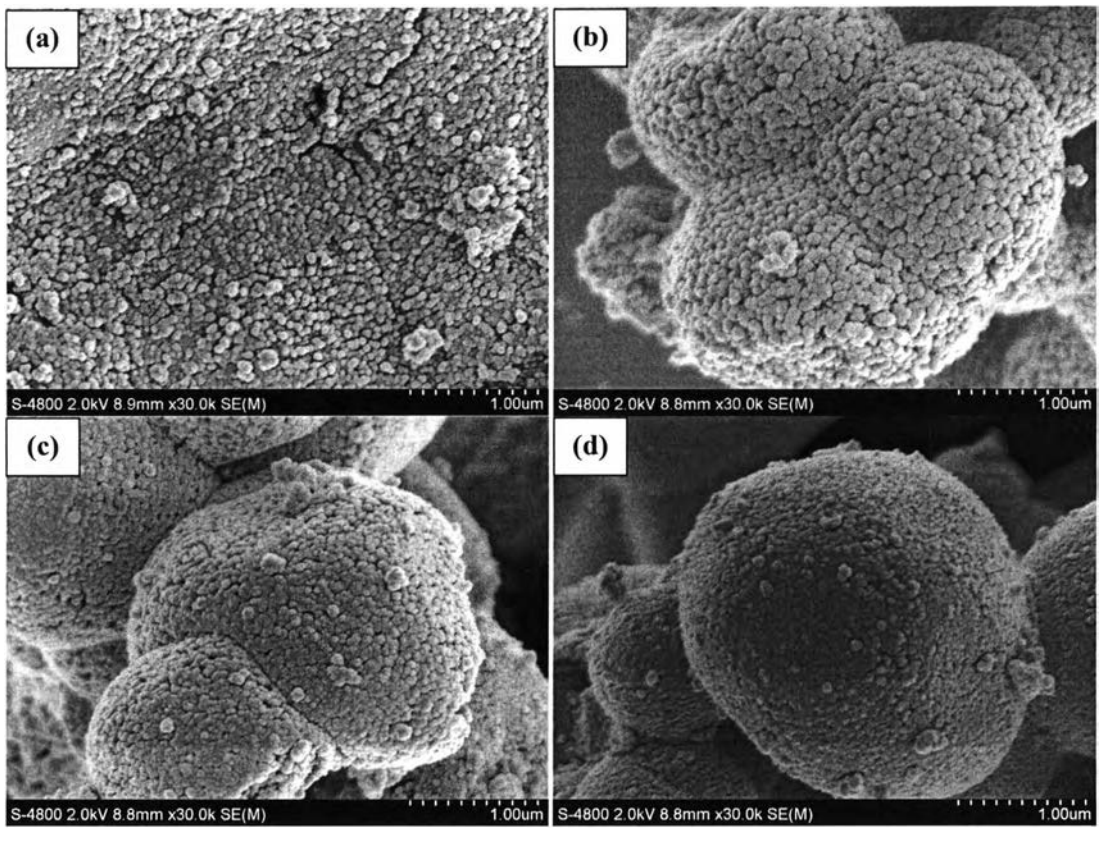

Figure 4.7 SEM images of a) ceria, and ordered mesoporous ceria at b) 1; c) 2 and d) 3 filling cycles.

To confirm the order of the mesoporous ceria structure, TEM was used to analyze. The mesoporous ceria (Fig. 4.8 a and b) are well ordered after removal of the silica template. Comparing the TEM image (Fig. 4.8b) with MCM-48 pores (Fig. 4.8c), the black area in Fig. 4.8b is similar to the black pores in Fig. 4.8c, indicating that the mesoporous ceria has the same ordered structure as MCM-48(J. Am. 2001).

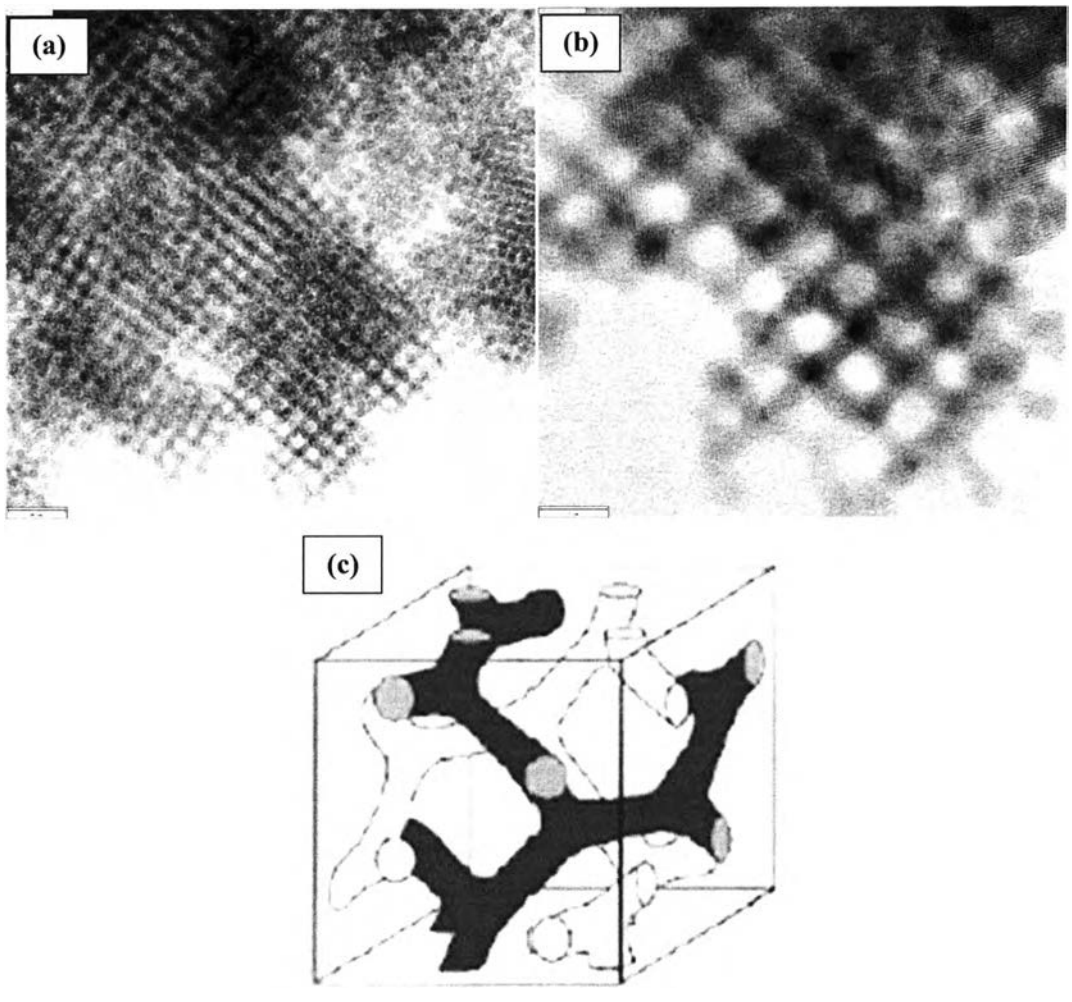

Figure 4.8 TEM images of the ordered mesoporous ceria a), b), and c) pores of MCM-48.

4.2 Temperature Programmed Reduction (TPR)

TPR experiments were conducted to investigate the reduction property of the nanocasting ceria. The TPR profiles of the ceria powder and the ordered mesoporous ceria are shown in Fig. 4.9. Two groups of the reduction peaks were observed. The first peak at low temperature from 350° to 650 °C is related to the reduction of the surface-capping oxygen of CeO_2 whereas the high temperature peak at 700°–850 °C is referred to the reduction of the bulk-phase lattice oxygen. The reduction of bulk oxygen occurs at higher temperature due to its higher thermal requirement to reduce Ce^{4+} to Ce^{3+}. The small reduction shoulder at 490° to 510 °C,

surface-capping oxygen, occurred from imperfections of the oxide surface, such as steps, kinks, and corners (Rao, 2003). The reduction mechanism was described by Rao in 1999, as shown in Fig. 4.10.

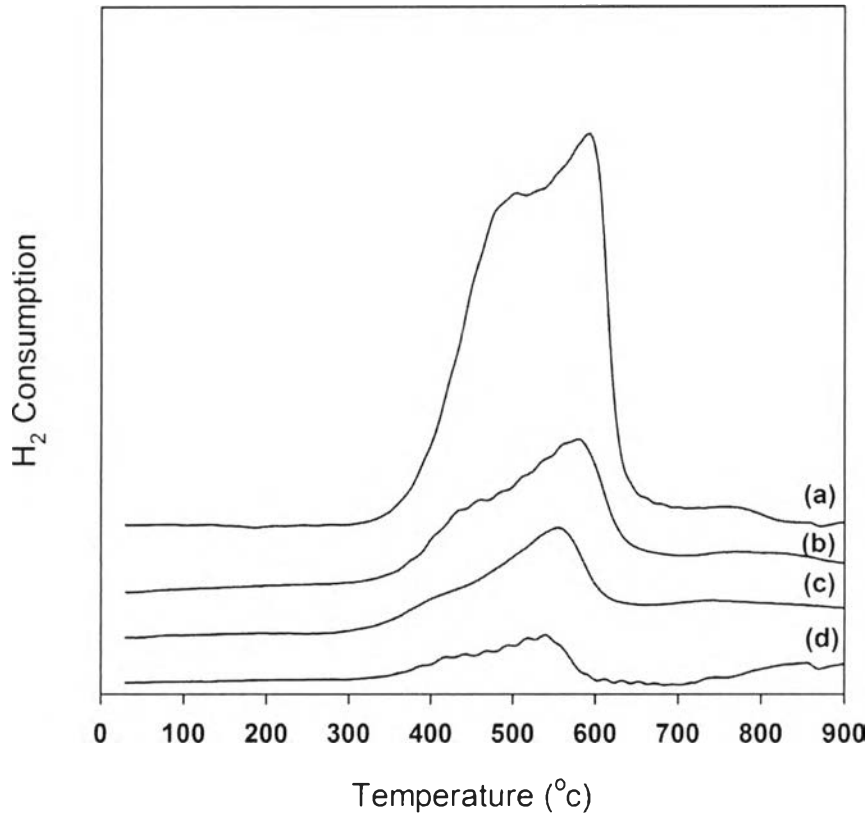

Figure 4.9 TPR profiles of ordered mesoporous ceria at (a) 1; (b) 2 and (c) 3 filling cycles (d) ceria powder.

The ceria reduction consists of four steps: (i) dissociation of hydrogen to form hydroxyl group on the surface of ceria, (ii) formation of anionic vacancies and reduction of neighboring Ce^{4+} to Ce^{3+}, (iii) desorption of water by recombination of hydrogen and hydroxyl groups, and (iv) diffusion of anionic vacancies from surface into the bulk.

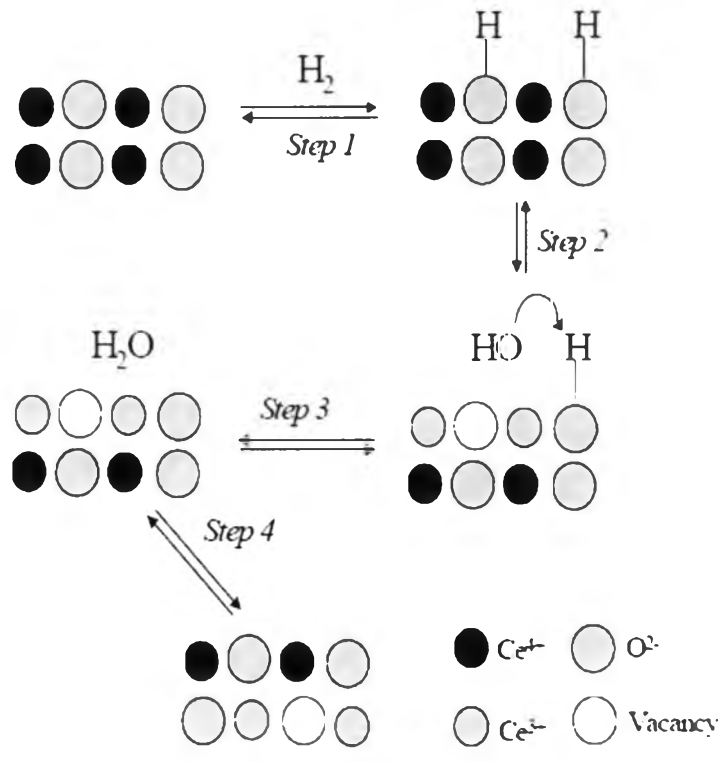

Figure 4.10 Schematic of ceria reduction (Rao, 2003).

The redox equation of ceria is shown below (Rogemond *et al.* 1997). The Ce^{3+}/Ce^{4+} redox cycle provides not only the unique redox properties, but also the ability to store and release oxygen via conversion between Ce^{3+} and Ce^{4+} oxidation state (Ji *et al.* 2008).

$$2\ CeO_2 + H_2 \longrightarrow Ce_2O_3 + H_2O$$

Although the TPR profiles of the ordered mesoporous ceria and the ceria powder are similar, but difference in the intensity of the low temperature peak is significantly distinguishable. Moreover, the peak intensity at the low temperature decreased with increasing the filling cycles. The highest intensity of the low temperature peak (Fig. 4.9a) was observed on the ordered mesoporous ceria obtained at 1 filling cycle. Areas under the peak correspond to the total gas consumption, implying that the ordered mesoporous ceria obtained from 1 filling cycle and having the highest surface area consumed the highest H_2 since the higher surface area

provides the higher amount of oxygen on the surface, resulting in higher amount of hydrogen absorbed to form hydroxyl group, as described by Rao in Fig. 4.10 (Rao, 1999).

As discussed previously that the second and the third filling cycles showed not only dense spherical morphology, but also less surface area, the TPR results thus indicated less H_2 consumption. This is the advantage for being a catalyst. That means, an improvement in the catalytic performance of the ceria structure can be achieved by increasing the surface area and the structure.